Solar-Terrestrial Physics. 2026, vol. 12, iss. 1, pp. 3–10. DOI: 10.12737/stp-121202601. © 2026 G.P. Mashnich, V.E. Tomin, V.A. Pulyaev. Published by INFRA-M Academic Publishing House

DOI: 10.12737/stp-121202601
EDN: FJNSCI

Received April 29, 2025
Accepted September 04, 2025

SPECTRAL OBSERVATIONS OF THE MOTIONS IN AND AROUND FILAMENT: TRANSVERSE OSCILLATIONS

G.P. Mashnich
Institute of Solar-Terrestrial Physics SB RAS, Irkutsk, Russia, mashnich@iszf.irk.ru

V.E. Tomin
Institute of Solar-Terrestrial Physics SB RAS, Irkutsk, Russia, tomin@iszf.irk.ru

V.A. Pulyaev
Institute of Solar-Terrestrial Physics SB RAS, Irkutsk, Russia, vasiliy_p@iszf.irk.ru

Abstract. The work based on spectral observations from Sayan Solar Observatory (SSO) is aimed at searching for signs that indicate a connection between oscillatory motions in the filament and the lower layers of the solar atmosphere. We also figure out on which scales transverse oscillations are detected in the filament. We analyze the simultaneously obtained time series of intensities and variations in the Doppler velocity in the photosphere (FeI λ 4897 Å) and in the chromosphere (Hβ λ 4861 Å) in the region of a large quiescent filament at its different positions on the Sun. In the distribution of the small-amplitude Doppler velocity oscillations beyond the filament and on its edge, we have found small areas, where wavelet spectra within 2–4 mHz in the chromosphere coincide with the wavelet spectra in the photosphere. In the filament transverse (horizontal) displacements in the sky plane, we have revealed oscillations of two types. Individual filament structures (about 2″–4″ in size) oscillate transversely within $5>f>1$ mHz at the 0.3–2.1 Mm displacement amplitude. The transverse oscillation spectra of the filament fragment at its position on the central meridian demonstrate two frequency ranges: $5>f>1$ mHz and ~0.5 mHz. There is only one peak (~0.26 mHz) in the spectrum when the filament moves away from the Sun's central meridian.

Keywords: solar photosphere, chromosphere, filament oscillations.

INTRODUCTION

Prominences are dense ($(3\div6)10^{11}$ cm^{-3}) cold features (~8000–12000 K) that are observed over the solar limb and can maintain equilibrium in the hot corona (~10^6 K) for a long time (see, e.g., [Tandberg-Hanssen, 1995]). On the disk, prominences show as dark elongated features called filaments. Shapes and dynamics of filaments/prominences are very diverse and are mainly determined by the magnetic field configuration. An important source of wave energy on the Sun is considered to be subphotospheric convection generating vortex flows and a wide spectrum of MHD oscillations. Deubner and Fleck [1989] investigated velocity and intensity variations, using lines formed in the photosphere and lower chromosphere. When analyzing difference spectra, the authors found large wave numbers in the frequency range 2–4 mHz, which agrees with the theoretical concepts of gravity wave properties and confirms their existence in the photosphere. Examining possible sources of chromospheric heating, Jefferies et al. [2006] have shown that inclined magnetic field lines at the boundaries of supergranulation cells (supergranules) provide "portals" through which magnetosonic waves with an oscillation frequency less than 5 mHz can propagate into the solar chromosphere. Kumar et al. [2023] have searched for signs of magnetosonic wave propagation in small-scale magnetic fields, using photospheric dopplerograms, calculated from SDO/HMI (Solar Dynamics Observatory/ Helioseismatic and Magnetic Imager) data, and chromospheric dopplerograms obtained in the CaII 8542 Å line with the Multi-Application Solar Telescope (MAST) of the Udaipur Solar Observatory. From wavelet analysis, Kumar et al. [2023] have found that the power of magnetosonic oscillations in the photosphere and chromosphere shows a good fit in the range 2.5–4 mHz. The results obtained by Kumar et al. [2023] illustrate propagation of oscillations (2.5–4 MHz) from the photosphere to the chromosphere along inclined magnetic field lines. According to Griffiths et al. [2018], global magnetosonic modes can either penetrate from the photosphere into the overlying atmosphere or propagate directly into the atmosphere along magnetic field lines, especially when these magnetic waveguides deviate from the vertical direction. These authors have calculated the power spectra of intensity oscillations in nine SDO/AIA (Atmospheric Imaging Assembly) bandwidths at randomly selected points: in an active region, on the quite Sun, and in a coronal hole during solar minimum. Griffiths et al. [2018] believe that strong 3- and 5-min oscillations in the power spectra found in all channels and selected regions on the Sun, as well as the results of their model calculations, can serve as evidence for the existence of a global oscillation excitation mechanism.

In quiescent and active filaments/prominences, small-amplitude oscillations are detected in features ranging in size from subsecond to several seconds. From observations

in various spectral lines, a wide range of periods has been identified for oscillations of small-amplitude filaments and prominences — from 1 min to 1 hr and more [Landman et al., 1977; Wiehr et al., 1984; Bashkirtsev, Mashnich, 1984; Tsubaki, Takeuchi, 1986; Balthasar et al., 1986; Molowny-Horas et al., 1997; Ning et al., 2009a, b]. High-resolution Hα images of the Sun [Lin et al., 2005] have suggested that filaments consist of numerous threads. The transverse size (0.2″) of fine threads is at the spatial resolution limit possible for ground-based observations. These fine threads reveal Doppler velocity variations and oscillatory motions across their axis in the plane of the sky [Lin et al., 2009; Lin, 2011]. In recent decades, many researchers have employed high spatial resolution data obtained with space observatory instruments [Hillier et al., 2013; Ofman et al., 2015; see the review by Arregui et al., 2018]. Hillier et al. [2013] have carried out a statistical study of transverse oscillations in a large number of threads of a quiescent prominence from Hinode/SOT (Solar Optical Telescope) high spatial resolution (0.1″) data. The authors detected oscillations with periods from 50 to 6000 s and with amplitudes from 0.2 to 23 km/s, and also indicated that the power spectrum of transverse oscillations of fine-thread elements in a quiescent prominence is consistent with the power spectrum of horizontal motions of photospheric magnetic fields. Ofman et al. [2015], also using Hinode/SOT data in the CaII and Hα lines, examined wave activity at a prominence foot and found quasi-periodic density oscillations propagating upward from the chromosphere into the prominence with typical periods 5–11 min and wavelengths <2000 km. Ofman and Kucera [2020] have identified these oscillations with nonlinear fast magnetosonic waves by comparing the model combined effect of nonlinear waves and fluxes on plasma with observed dynamics of motions in a prominence. Statistically significant analysis of filament oscillations of various types and their properties during high solar activity has been made by Luna et al. [2018], applying daily Hα data from GONG (Global Oscillation Network Group) for the period from January to June 2014. The oscillations were classified by amplitude: small-amplitude with velocities lower than 10 km/s and large-amplitude with velocities higher than 10 km/s. The average period 58±15 min was determined for oscillations of both types, and the averaged angle between motion direction and filament body is ~27°. This angle is consistent with the observed direction of filament magnetic fields [Leroy, 1987; Tandberg-Hanssen, 1995].

Our work is based on spectral observation data with spatial resolution 1″–1.5″ from Sayan Solar Observatory (SSO). The data set was obtained simultaneously in the photosphere (FeI λ 489.7 nm) and chromosphere (Hß λ 486.1 nm) in the vicinity of a large quiescent filament. The purpose of this paper is to analyze the interrelationships between photospheric and chromospheric motions and oscillations in a filament and its surroundings, as well as to explore the direction of oscillatory motions in the filament.

1. OBSERVATIONS AND PROCESSING

The observations were made with the SSO Automated Horizontal Solar Telescope [Osak et al., 1979]. The telescope feeding the spectrograph consists of a ceolostat, a main spherical mirror of diameter 80 cm and focal length 20 m. The photoelectric guide compensates for rotation and keeps the solar image on the spectrograph slit up to 1″. The width of the spectrograph slit corresponds to 1″ on the solar surface, but the actual spatial resolution is often limited by visibility conditions to ~1.5″–2″. The automated control system of the telescope allows us to manage the instrument and set observation parameters. To record the spectra, we have employed a FLI ProLine camera with a matrix 1024×1024 px of size 24 μm. The sensor size 24.5×24.5 mm makes it possible to place a spectral region of ~8 Å along the dispersion in the V order. We used the spectral range 4857–4865 Å with photospheric FeI 4859 Å and chromospheric Hß 4861 Å lines.

For the analysis, we chose a large quiescent filament in the northern hemisphere during its second passage through the solar disk in June 2023. Coronal holes were located to the east and west of the filament (Figure 1, *a*). To visually examine possible sources of oscillations in the filament, we employed SDO/AIA data for time intervals including 1 hr before observations and the time of observations. During these time intervals, no brightening, jets, nanoflares, EIT waves, or other oscillation triggers were detected near the filament

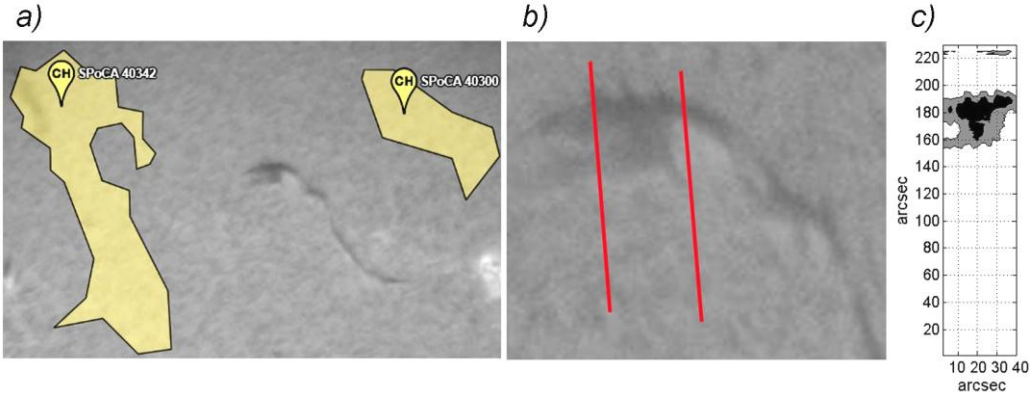

Figure 1. Location of the filament and coronal holes on the disk according to [http://helioviewer.org] as observed on June 26, 2023 at 00:45 UT (*a*); an Hα filament image on June 26, 2023 at 00:45 UT according to GONG data, red lines mark the scan area (*b*); filament fragment in the Hβ line according to our spectral observation data on June 26, 2023 00:57 UT (*c*)

on all observation days [Tripathi et al., 2009]. Note that during the first passage through the Sun's disk in May 2023, the filament partially erupted twice and subsequently recovered. Data is collected by scanning, i.e. taking a series of spectrograms by stepping a solar image along the spectrograph slit. The region including the filament fragment is scanned with a cadence of 57 s and with a spatial step of 2″. The length of the slit corresponds to 230″ on the solar surface. Each scan contains 20 frames (spectrograms obtained with an exposure of 0.1 s). With the binning and the spatial step, the scan area was 40″×230″. Here we analyze series of scans obtained on June 26, 2023 for a filament fragment with coordinates E00N33, when the filament was on the central meridian, and on June 28, 2023 for a filament fragment with coordinates W25N33. We have selected series of length 145 min (00:34–02:59 UT) on June 26, 2023 and 179 min (00:09–03:06 UT) on June 28, 2023, recorded under the best observation conditions. Before processing a series of spectrograms, an averaged base frame is created [Mashnich et al., 2009; Mashnich, Kiselev, 2019]. The Doppler velocity is defined as the displacement of the center of the median of the working line profile from a fixed position in the base frame in each row of the spectrogram. The Hβ line with a half-width of 4.2 Å is generally formed in the chromosphere, where the magnetic pressure dominates the gas pressure [Zhang, 2023]. To exclude the contribution of the chromosphere, we usually calculate the Doppler velocity near the core of the Hβ line at a distance ±(0.4–0.45) Å from the line center.

To identify transverse oscillations, we adopt the method of the lowest line intensity [Mashnich et al., 2012]. With this method, we suppose that the conditions for the formation of the Hβ line in a quiescent filament change slightly during observations. Referring to Figure 2, *a*, the minimum Hβ line intensity along the spectrograph slit clearly defines the position of the filament on the slit. With a fixed position of the filament on the spectrograph slit, the processing program finds the pixel number with minimum intensity in each frame of the time series of spectra, forming a time series of filament displacements in projection onto the plane of the sky (see Figure 2, *b*). Using the data, we estimate the amplitude of filament displacements.

When searching for filament transverse motions in projection onto the plane of the sky, another method of processing spectrograms obtained in scanning mode is applied. We choose the matrix row located in the filament (Figure 3, red horizontal lines). A 2D time–distance diagram is constructed by extracting intensity and Doppler velocity values in the given matrix row along the scanning direction in each scan (time step). The intensity diagrams show the position of a filament fragment in the given matrix row during observations. For the given matrix row, we also draw diagrams of chromospheric and photospheric Doppler velocities (see Figure 7).

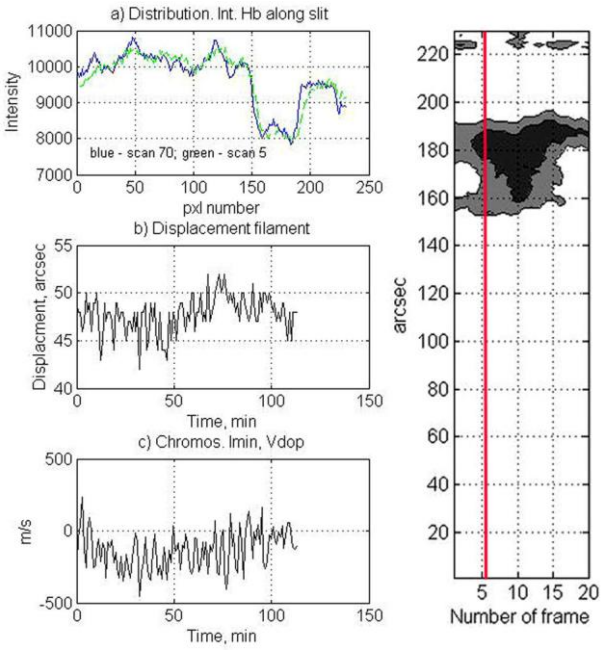

Figure 2. Intensity distribution of the Hβ line along the spectrograph slit (*a*) in the fifth scan frame (indicated by the red vertical line in panel *d*) at different scanning stages; green and blue colors are intensity profiles in the 5th and 70th scans respectively. Filament displacement in projection onto the plane of the sky as function of time (*b*). Doppler velocities in the chromosphere of the filament at points with minimum intensity (*c*). Intensity map of the scanned area (*d*)

2. RELATIONSHIP BETWEEN MOTIONS OF PHOTOSPHERIC AND CHROMOSPHERIC PLASMA

Space-time data acquired by scanning a region on the Sun allows us to analyze intensity and velocity time series at each point in this region. From the calculation results, we constructed maps of intensity and Doppler velocity distribution in the region of 40″×230″, which includes a filament fragment. For example, Figure 3 presents maps of spatial distribution of intensity and Doppler velocities in the chromosphere and photosphere for a single scan. When watching a video compiled from consecutive scans, we can see that hills of Doppler velocity knock together, merge, and separate, gradually changing signs.

To analyze photospheric and chromospheric oscillations, we used time series of the Hβ-line intensity and Doppler velocity in the chromosphere and photosphere at each point of the scan of the spatiotemporal image series. From the results of Fourier analysis of time series for various frequency ranges, we drew oscillation distribution maps, which show the spatial localization of peaks at a power level of 0.7. In the filament region, oscillation distributions feature areas with characteristic filament/prominence oscillations in frequency ranges 0.24–0.26 mHz (~60 min), 0.6–0.8 mHz (20–25 min), and 1.3–0.8 mHz (10–13 min). In our work, we deal with oscillations in the frequency range 2–4 mHz, which are localized in the same areas on the maps of oscillation distributions in the chromosphere and in the photosphere. In Figure 4, blue

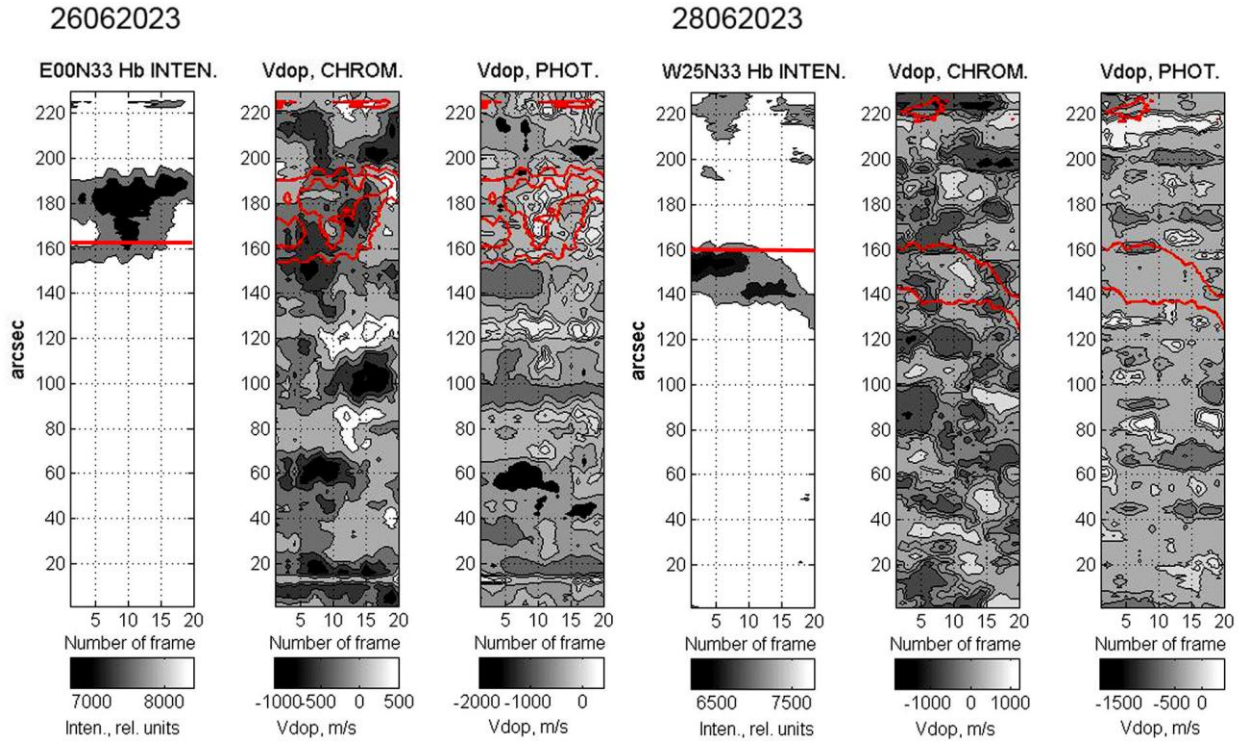

Figure 3. Maps of intensity distribution of the Hβ line (left) and the Doppler velocity in the chromosphere (middle) and photosphere (right) in a scan area on June 26 (*a*) and 28 (*b*), 2023. Red contours outline the position of the filament with a 50–60 % Hβ-line intensity level. Red horizontal lines denote the matrix rows for which space-time diagrams of intensity and velocity are drawn to determine transverse oscillations in the plane of the sky

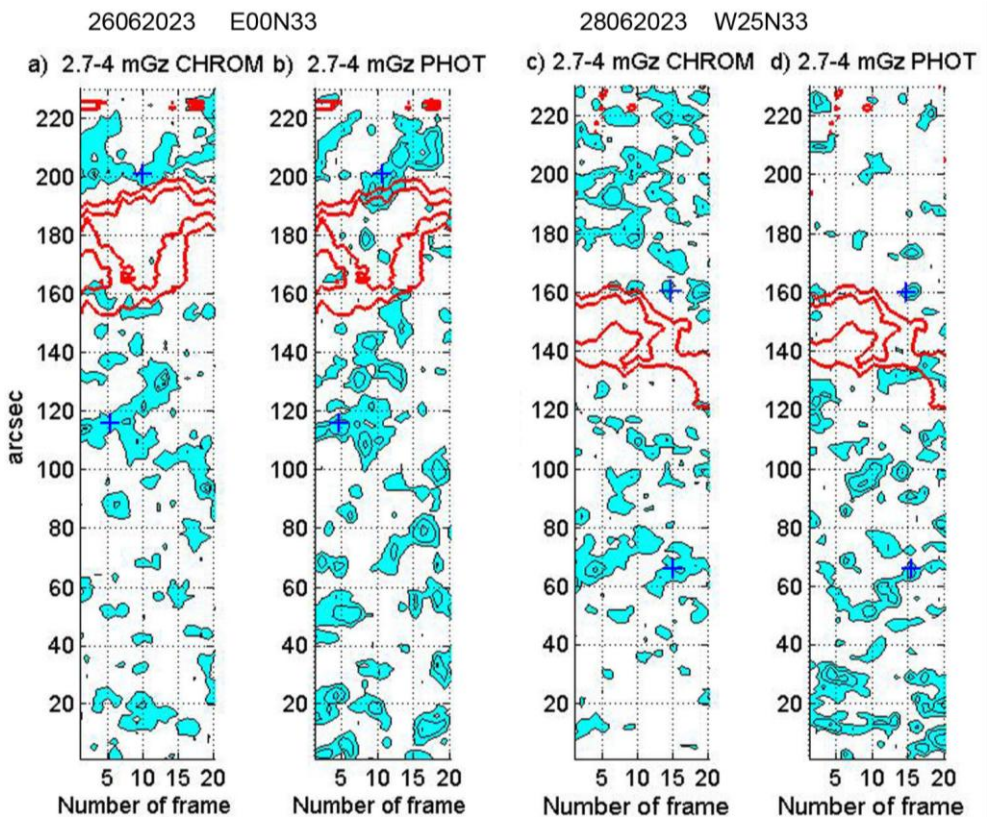

Figure 4. Distribution of oscillations in the frequency range 2.7–4 mHz in the filament and its surroundings in the chromosphere (*a*, *c*) and photosphere (*b*, *d*) on June 26 (left) and 28 (right), 2023 at the 0.7 maximum power spectrum at this frequency. Red contours denote the location of the filament; blue crosses mark the places of spatial coincidence of the frequency spectrum of oscillations in the photosphere and chromosphere at the edges of the filament and outside it, the wavelet spectra for which are shown in Figures 5, 6

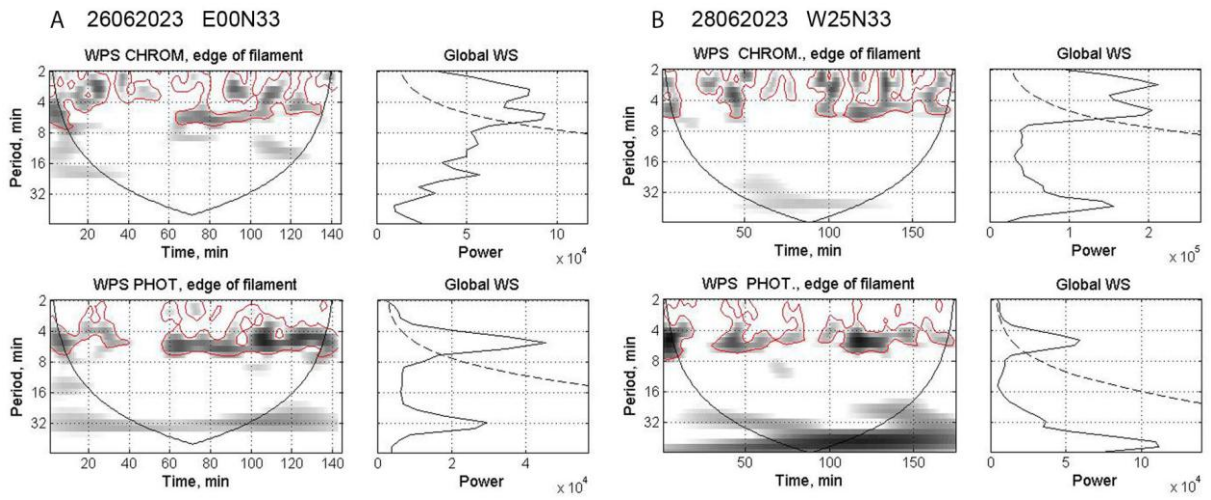

Figure 5. Wavelet analysis of Doppler velocity time series at the filament edge in the chromosphere (top) and photosphere (bottom) from observations on June 26 (*a*) and 28 (*b*), 2023. In power spectra (left panels), the most powerful periodic component is highlighted in black and gray with a red contour that corresponds to an 85 % confidence level; in global spectra (right panels), a dashed line indicates a 95 % confidence level

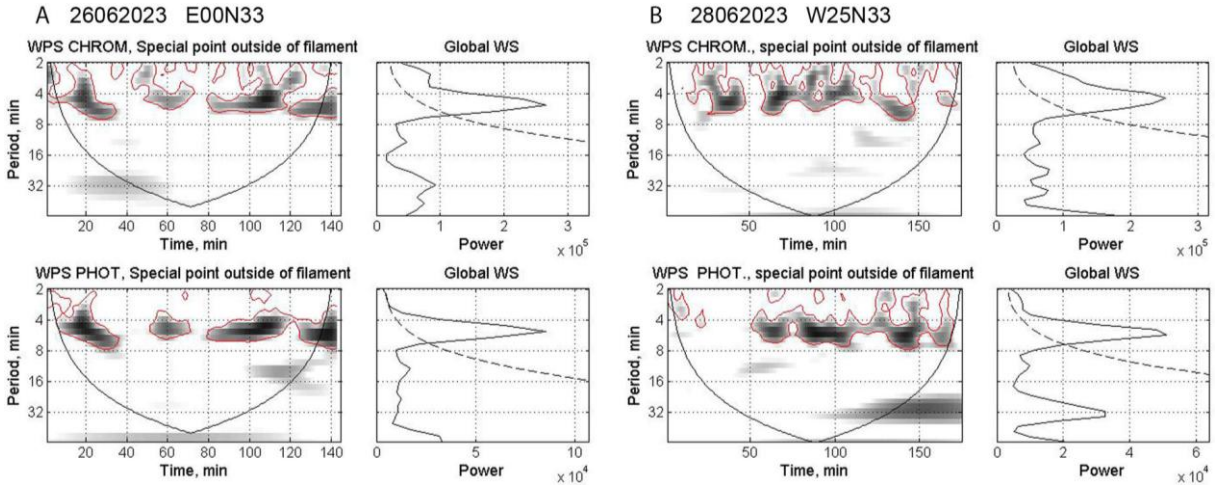

Figure 6. The same as in Figure 5 for exceptional points outside the filament

crosses mark the places of spatial coincidence of the frequency spectrum of Doppler velocity oscillations in the photosphere and chromosphere outside the filament and at its edges, the wavelet spectra for which are displayed in Figures 5 and 6. The wavelet analysis [Torrence, Compo, 1998] makes it possible to trace the time variation in the power of oscillation spectra and identify nonstationary phenomena in the parameters under study.

At the filament edge, a wide maximum with a frequency f>2 mHz is divided into two peaks of ~3 and ~5 mHz (Figure 5). In detail, the time structures of the wavelet spectra of photospheric and chromospheric oscillations in the range 3–3.5 mHz largely coincide. The maps of ~3 mHz oscillation power distribution clearly show that the oscillation power is suppressed at the location of the filament (see Figure 4, *a*, *b*). This may be explained by the fact that the oscillations with f>2 mHz are intrinsic to the fine structures filling the filament body. It is assumed (see, e.g., [Lin et al., 2009; Lin, 2011; Mashnich et al., 2009]) that a multitude of fibrils with slightly different speeds, amplitudes, and phases of oscillations are integrated in the line of sight. The difference between these parameters is determined by local conditions. The density at filament edges decreases, which makes it possible to resolve individual fine structures, which make up the filament, and measure characteristics of their oscillations. We also found small areas of spatial coincidence of photospheric and chromospheric Doppler velocity oscillations in the frequency range 2–4 mHz in distributions of oscillations outside the filament. A correlation between time variations in the power of the wavelet spectra, chromospheric and photospheric Doppler velocities was found from observational data on June 26, 2023. Furthermore, ~3.5 mHz peaks in the global wavelet spectra of the photosphere and chromosphere coincide (see top and bottom right panels in Figure 6, *a*). Chromospheric wavelet spectra also indicate that there are chromospheric oscillations with ~5 mHz frequency. We have received results similar to those presented in Figure 6, *a* in other places of spatial coincidence of the distributions of photospheric and chromospheric oscillations. The region in question moved 25° west of the central meridian on June 28, 2023. In this case, in the photospheric and chromospheric

wavelet spectra a time coincidence of power is detected during some observation periods (see Figure 6, *b*) with a slight divergence between peaks in the global wavelet spectra of the chromosphere (4 mHz) and photosphere (3.5 mHz).

3. FILAMENT TRANSVERSE OSCILLATIONS

On June 26, 2023, the filament was on the central meridian, the spectrograph slit was perpendicular to the filament body. The location of the filament on the central meridian is preferable when examining transverse oscillations relative to the filament body in the plane of the sky as it eliminates most projection effects. The component of filament transverse motions in the plane of the sky (in the horizontal plane) relative to its axis can be determined from the minimum intensity of the spectral line along the spectrograph slit for one-dimensional observations (vertical red line in the right panel of Figure 2). We build time series of filament displacements in each frame and analyze horizontal transverse oscillations of filament details ~2″. Displacement amplitudes in the range 0.3–2.1 Mm and oscillation periods 200–990 s were derived from data on 20 frames. These results check well with the data on transverse oscillations of fine threads (0.1″) of the filament (see, e.g., [Hillier et al., 2013]). Detecting filament fragment transverse motions in a series of spectra obtained by scanning is not a trivial task. When processing a series of scans, we draw a two-dimensional time–distance diagram by extracting the Hβ intensity and the Doppler velocity in the photosphere and chromosphere in a given matrix row in each scan. Figure 7 exhibits diagrams for the matrix rows indicated by red horizontal lines in Figure 3.

Hβ-line intensity variations in the time–distance diagram (see Figure 7) represent horizontal transverse motions of the entire filament fragment relative to the given matrix row. The periodic change of sign on the velocity field maps in the frame probably indicates spiral motions. It is known from polarimetric measurements of the magnetic field in quiescent prominences [Leroy et al., 1984; Orozco Suárez et al., 2014] that the magnetic field vector makes an angle 20°–30° with the filament axis. The same angles between the filament axis and the direction of motion for oscillations of all types were found from statistical analysis of a large number of observations by Luna et al. [2018].

The time series of intensity variations in Figure 8 were derived from local intensity values in the time–distance diagram, identified in frames near the filament edge. After removing the intensity of the linear trend, caused by a change in the height of the Sun above the horizon, from the time series, the wavelet analysis was applied to them to determine periodicities in filament horizontal transverse motions. According to observations on June 26, 2023 (see Figure 8, *a*), significant periods of transverse filament oscillations are identified in two ranges: $5>f>1$ mHz and ~0.5 mHz (30 min). When the filament moves away from the central meridian on June 28, 2023 (see Figure 8, *b*), there was one peak of ~0.26 mHz (64 min) in the wavelet spectrum. No attenuation of long-period transverse oscillations was detected during our observations. In the model of global transverse oscillations and stable quiescent prominence, Kolotkov et al. [2016] consider the prominence as a direct wire with current. Kolotkov et al. [2016] call the oscillations of the structure as a whole "global", in contrast to the oscillations of individual fibrils. Properties of both vertical and horizontal oscillations depend on the density and height of a prominence above the photosphere and the amount of current in it. A prominence can be simultaneously resistant to oscillations in both directions when the

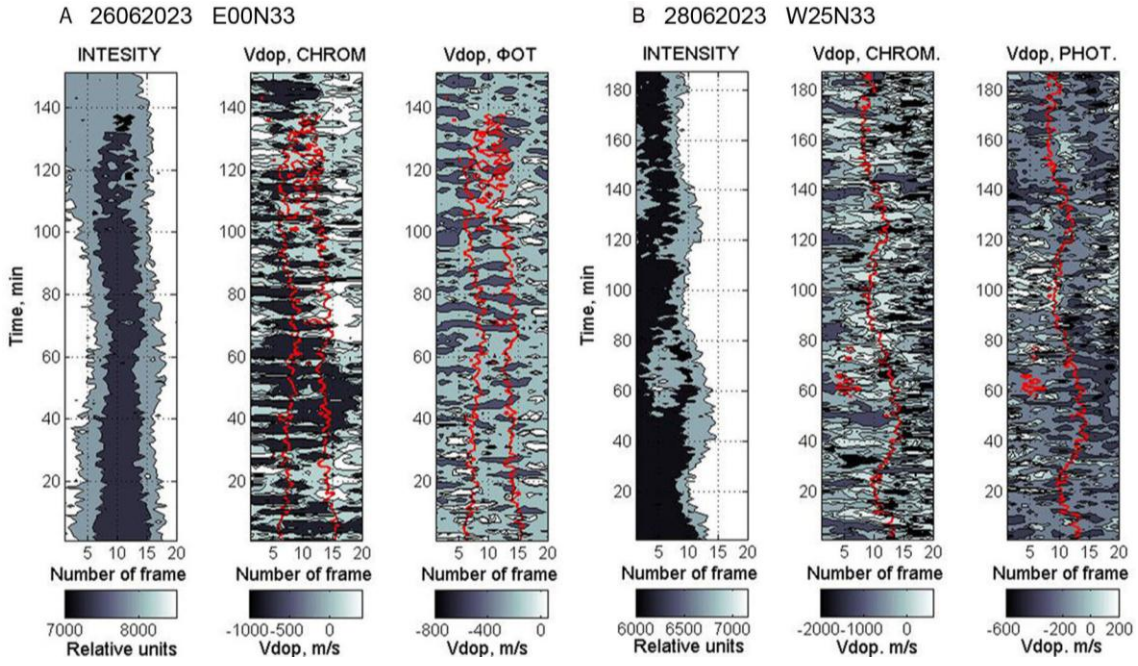

Figure 7. Time intensity variations showing the location of the filament fragment (left panels) and time series of the Doppler velocity in the chromosphere (middle panels) and photosphere (right panels) in a given matrix row, as observed on June 26 (*a*) and 28 (*b*), 2023.The matrix rows for which the time–distance diagrams are drawn are indicated by horizontal red lines in left panels of Figure 3

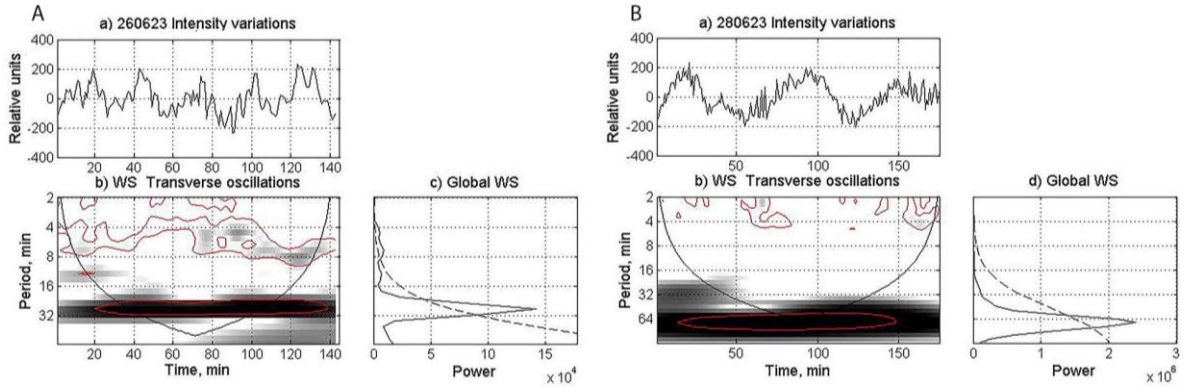

Figure 8. Intensity variations obtained from observations on June 26 (*a*) and 28 (*b*), 2023, associated with shear motions of the filament relative to its axis (top); wavelet power spectra of transverse oscillations (bottom left); the red contour is an 85 % confidence level; global power spectrum (bottom right); the dashed line indicates a 95 % confidence level

current in it is stronger than in photospheric sources, and its height is less than half the distance between them. In this model, vertically and horizontally polarized oscillations are unrelated, and the oscillation periods in both directions are independent.

4. DISCUSSION

Using spectral scans of a filament region 40″×230″, we simultaneously obtain time series of intensity and Doppler velocity in the photosphere and chromosphere in and outside the filament. The spatial resolution allows us to detect collective oscillations averaged over a 1″×2″ region. In power distribution of Doppler velocity oscillations in the frequency range 2–4 mHz, small areas have been revealed at the edges of the filament and outside it, where photospheric and chromospheric oscillations are localized at a time. We have found that the correlation between time variations in photospheric and chromospheric Doppler velocity wavelet spectra in the frequency range 2–4 mHz is manifested at the filament edges. This is consistent with the results obtained with higher resolution [Ofman et al., 2015; Ofman, Kucera, 2020]. We have got the same range of oscillation periods, but the amplitude values are smaller. We have also identified an unambiguous correlation between time variations in the power of chromospheric and photospheric Doppler velocity wavelet spectra in the frequency range 2–4 mHz outside the filament at exceptional points of spatial coincidence of oscillations. This result concur with the conclusions drawn in [Kumar et al., 2023], where observational evidence was given that the periodic nature of the interaction of acoustic waves in the convective zone with background magnetic fields is responsible for the occurrence of episodic oscillations in the photosphere and chromosphere. The correlation between time variations in the power of photospheric and chromospheric wavelet spectra of velocity oscillations, which we have discovered, suggests that photospheric oscillations can penetrate into the chromosphere and filament. This possibility is discussed in the literature (see, e.g., [Deubner, Fleck, 1989; Jefferies et al., 2006; Ofman et al., 2015;Griffiths et al., 2018]). Small-scale and large-scale oscillations have been detected in filament transverse motions in the plane of the sky. Some filament details (~2″) execute transverse oscillations in the frequency range 5>*f*>1 mHz with an amplitude 0.3–2.1 Mm. With a filament fragment on the central meridian, the transverse oscillation spectra exhibit two frequency ranges: 5>*f*>1 mHz and about 0.5 mHz. When the filament moves away from the central meridian, there is only one peak of ~0.26 mHz in the spectrum. Transverse and Doppler velocity oscillations are simultaneously observed in the filament.

CONCLUSION

1. In the photosphere and chromosphere at the edges of the filament and outside it, we have found a spatial coincidence of small regions in the power distributions of chromospheric and photospheric Doppler velocity oscillations in the frequency range 2–4 mHz.
2. We have revealed a correlation between periodic variations in the power of photospheric and chromospheric Doppler velocity wavelet spectra at the filament edge and outside it in the 2–4 mHz range. The time coincidence of the details of these spectra is well-defined when the filament is located on the central meridian.
3. Transverse (horizontal) oscillations relative to the filament axis with periods 200–990 s and displacement amplitudes in the range 0.3–2.1 Mm were recorded in filament structures of ~2″.
4. We have proposed a method for determining transverse motions of large filament fragments in the plane of the sky from spectral observations. Using this method, we recorded transverse oscillations of a filament fragment with periods of several tens of minutes.
5. Transverse and Doppler velocity oscillations are simultaneously observed in the filament.

Observational studies of small-amplitude intensity and Doppler velocity oscillations contribute to understanding the relationship between photospheric and chromospheric oscillations, which is necessary for modeling wave propagation from the photosphere to a filament.

We are grateful to the reviewers for their critical comments and suggestions on how to improve the paper. We also thank the SDO/AIA and GONG teams for providing access to the databases via the Internet. The observations were made using the equipment of Shared Equipment Center «Angara» [http://ckp-rf.ru/ckp/3056].

REFERENCES

Arregui I., Oliver R., Ballesteret J.L. Prominence oscillations. *Living Rev. Solar Phys*. 2018, vol. 15, no. 3. DOI: 10.1007/s41116-018-0012-6.

Balthasar H., Knoelker M., Wiehr E., Stellmacher G. Evidence for quasi-periodic Doppler motions in solar prominences. *Astron. Astrophys.* 1986, vol. 163, no. 1-2, pp. 343–346.

Bashkirtsev V.S., Mashnich G.P. Oscillatory processes in prominences. *Solar Phys*. 1984, vol. 91, pp. 93–101. DOI: 10.1007/BF00213616.

Deubner F.-L., Fleck B. Dynamics of the solar atmosphere I-Spatio-temporal analysis of waves in quiet solar atmosphere. *Astron. Astrophys*. 1989, vol. 213, pp. 423–428.

Griffiths M.R., Fedun V., Erdélyi R., Zheng R. Solar atmosphere waves dynamics generated by solar global oscillating eigenmodes. *Adv. Space Res*. 2018, vol. 61, iss. 2, pp. 720–737.DOI: 10.1016/j.asr.2017.10.053.

Hillier A., Morton R.J., Erdélyi R.A. Statistical study of transverse oscillations in a quiescent prominence. *Astrophys. J. Lett*. 2013, vol. 779, no. 2, p. 16. DOI: 10.1088/2041-8205/779/2/L16.

Jefferies S.M., McIntosh S.W., Armstrong J.D., et al. Magnetoacoustic portals and the basal heating of the solar chromosphere. *Astrophys. J. Lett*. 2006, vol. 648, no. 2, pp. 151–155. DOI: 10.1086/508165.

Kolotkov D.Y., Nisticò G., Nakariakov V.M. Transverse oscillations and stability of prominences in a magnetic field dip. *Astron. Astrophys*. 2016, vol. 590, p. 120. DOI: 10.1051/0004-6361/201628501.

Kumar H., Kumar B., Rajaguru S.P., et al. A study of the propagation of magnetoacoustic waves in small-scale magnetic fields using solar photospheric and chromospheric Dopplergrams: HMI/SDO and MAST observations. *J. Atmos. Solar-Terr. Phys.* 2023, vol. 247, p. 106071. DOI: 10.1016/j.jastp.2023.106071.

Landman D.A., Edberg S.J., Laney C.D. Measurements of Hβ, He D3, and Ca+ λ8542 line emission in quiescent prominences. *Astrophys. J.* 1977, vol. 218, pp. 888–900. DOI: 10.1086/155744.

Leroy J.L. Observation of prominence magnetic fields. *Proc. of the Workshop "Dynamics and Structure of quiescent solar prominences"*. Palma de Mallorca, Spain, 1987, pp. 77–113. DOI: 10.1007/978-94-009-3077-3_13.

Leroy J.L., Bommier V., Sahal-Brechot S. New data on the magnetic structure of quiescent prominences. *Astron. Astrophys*. 1984, vol. 131, no. 1, pp. 33–44.

Lin Y. Filament thread-like structures and their small-amplitude oscillations. *Space Sci. Rev*. 2011, vol. 158, pp. 237–266. DOI: 10.1007/s11214-010-9672-9.

Lin Y., Engvold O., Rouppe van der Voort L., et al. Thin threads of solar filaments. *Solar Phys*. 2005, vol. 226, pp. 239–254. DOI: 10.1007/s11207-005-6876-3.

Lin Y., Soler R., Engvold O., et al. Swaying threads of a solar filament. *Astrophys. J.* 2009, vol. 704, pp. 870–876. DOI: 10.1088/0004-637X/704/1/870.

Luna M., Karpen J., Ballester J.L., et al. GONG catalog of solar filament oscillations near solar maximum. *Astrophys. J. Suppl Series* 2018, vol. 236, pp. 35–65. DOI: 10.3847/1538-4365/aabde7.

Mashnich G.P., Kiselev A.V. Spectral observations of the eruption of a filament. *Astronomy Rep.* 2019, vol. 63, no. 7, pp. 608–617. DOI: 10.1134/S1063772919070060.

Mashnich G.P., Bashkirtsev V.S., Khlystova A.I. Spatial distribution of oscillations in filaments. *Geomagnetism and Aeronomy.* 2009, vol. 49, no. 7, pp. 891–897. DOI: 10.1134/S0016793209070111.

Mashnich G.P., Bashkirtsev V.S., Khlystova A.I. Small-Amplitude Oscillations in Solar Filaments. *Astronomy Reports.* 2012, vol. 56, no. 3, pp. 241–249. DOI: 10.1134/S1063772912030055.

Molowny-Horas R., Oliver R., Ballester J.L., Baudin F. Observations of Doppler oscillations in a solar prominence *Solar Phys*. 1997, vol. 172, pp. 181–188. DOI: 10.1023/A:1004922809950.

Ning Z., Cao W., Goode P.R. Behavior of the spines in a quiescent prominence observed by Hinode/SOT *Astrophys. J.* 2009a, vol. 707, pp. 1124–1130. DOI: 10.1088/0004-637X/707/2/1124.

Ning Z., Cao W., Okamoto T.J., et al. Small-scale oscillations in a quiescent prominence observed by HINODE/SOT: Prominence oscillations. *Astron. Astrophys*. 2009b, vol. 499, pp. 595–600. DOI: 10.1051/0004-6361/200810853.

Ofman L., Kucera T. Fast magnetosonic waves and flows in a solar prominence foot: Observations and modeling. *Astrophys. J*. 2020, vol. 899, no. 2, pp. 99–109. DOI: 10.3847/1538-4357/aba2eb.

Ofman L., Knizhnik K., Kucera T., Schmieder B. Nonlinear MHD waves in a prominence foot. *Astrophys. J*. 2015, vol. 813, pp. 124–135.DOI: 10.1088/0004-637X/813/2/124.

Orozco Suárez D., Asensio Ramos A., Trujillo Bueno J. The magnetic field configuration of a solar prominence inferred from spectropolarimetric observations in the HeI 10 830 Å triplet. *Astron. Astrophys*. 2014, vol. 566, A46. DOI: 10.1051/0004-6361/201322903.

Osak B.F., Grigoryev V.M., Kruglov V.I., Skomorovsky V.I. The Automated Solar Telescope. *Novaya tekhnika v astronomii* [New Machinery in Astronomy]. 1979, vol. 6, pp. 84–90. (In Russian).

Tandberg-Hanssen E. *The Nature of Solar Prominences.* Dordrecht, Kluwer, 1995, 413 p. DOI: 10.1007/978-94-017-3396-0.

Torrence C., Compo G.P. A practical guide to wavelet analysis. *Bull. Americ. Meteorolog. Soc*. 1998, vol. 79, pp. 61–78. DOI: 10.1175/1520-0477(1998)079<0061:APGTWA>2.0.CO;2.

Tripathi D., Isobe H., Jain R. Large amplitude oscillations in prominences. *Space Sci. Rev*. 2009, vol. 149, pp. 283–298. DOI: 10.1007/s11214-009-9583-9.

Tsubaki T., Takeuchi A. Periodic oscillations found in the velocity field of a quiescent prominence. *Solar Phys*. 1986, vol. 104, pp. 313–320. DOI: 10.1007/BF00159084.

Wiehr E., Balthasar H., Stellmacher G. Oscillations of the Hα emission in solar prominences. *Solar Phys.*, 1984, vol. 94, pp. 285–288. DOI: 10.1007/BF00151318.

Zhang H. *Solar Magnetism.* Singapore, Springer Nature Singapore, 2023, pp. 91–101.DOI: 10.1007/978-981-99-1759-4.

URL: http://Helioviewer.org (accessed July 3, 2025).

URL: http://ckp-rf.ru/ckp/3056/ (accessed July 3, 2025).

Original Russian version: Mashnich G.P., Tomin V.E., Pulyaev V.A., published in Solnechno-zemnaya fizika. 2026, vol. 12, no. 1, pp. 5–13. DOI: 10.12737/szf-121202601.

How to cite this article

Mashnich G.P., Tomin V.E., Pulyaev V.A. Spectral observations of the motions in and around filament: Transverse oscillations. *Sol.-Terr. Phys*. 2026, vol. 12, iss. 1, pp. 3–10. DOI: 10.12737/stp-121202601.